

Electronic Supplementary Information

TiO₂-B Nanorods on Reduced Graphene Oxides as Anode Materials for Li Ion Batteries

Mengmeng Zhen,^a Shengqi Guo,^a Guandao Gao,^a Zhen Zhou,^{*b} Lu Liu^{*a}

^aTianjin Key Laboratory of Environmental Remediation and Pollution Control, College of Environmental Science and Engineering, Nankai University, Tianjin 300071, P.R. China.

^bTianjin Key Laboratory of Metal and Molecule Based Material Chemistry, Key Laboratory of Advanced Energy Materials Chemistry (Ministry of Education), Institute of New Energy Material Chemistry, Collaborative Innovation Center of Chemical Science and Engineering (Tianjin), Nankai University, Tianjin 300071, P.R. China.

Experimental Section

Preparation of GO Nanosheets.

All the reagents are of analytic grade and were used without any purification. GO nanosheets were prepared via the oxidation of graphite by using the improved Hummers' method. In detail, graphite powder (2.0 g) was dispersed into 100 ml cooled (0 °C) H₂SO₄ (98%), and KMnO₄ (6.0 g) was slowly added into the mixture under vigorous agitation. Then, the resultant solution was continually stirred at 35 °C for 3 days. Afterwards, 200 ml distilled water was added and kept at 98 °C for 2 h. After the solution was cooled to 60 °C, 10 ml H₂O₂ (30%) was injected into the suspension to completely react with the excess KMnO₄. The suspension was centrifuged and washed with HCl (30%) and distilled water until the pH value was ~7. The precipitate was collected and stored for further use.

Preparation of TiO₂-B/RGO Nanorods.

In a typical synthetic procedure, 4 mL TBT was dispersed into KOH solution (10 M, 40 mL), followed by vigorous agitation for 1 h. The mixture was placed into a 50 mL Teflon-lined autoclave and maintained at 180 °C for 48 h. After naturally cooled to room temperature, the obtained products were centrifuged and washed with 0.1 M HCl solution and distilled water until the pH value was ~7, and then dried at 60 °C in vacuum for 10 h, resulting in the production of an intermediate. The as-prepared intermediate (0.2 g) and GO (10 g/L, 2 mL) were added into a HCl solution (0.1 M, 40 mL) under vigorous agitation. The mixture was transferred into a 50 mL Teflon-lined autoclave and kept at 180 °C for 6 h. After naturally cooled to room temperature, the obtained precipitates were separated from the solution by centrifugation and subsequently washed with deionized water and then dried at 60 °C and annealed at 400 °C for 2 h under argon, resulting in the final product.

Materials Characterization.

The obtained samples were characterized by X-ray diffraction (XRD, Rigaku D/Max III diffractometer with Cu K α radiation, λ = 1.5418 Å), scanning electron microscope (SEM, Nova Nano SEM 230), transmission electron microscope (TEM, Tecnai G2F20, FEI), high-resolution TEM (HRTEM, Tecnai G2F20, FEI), and atomic force microscope (AFM, MMAFM/STM, D3100M, Digital Ltd.), and thermogravimetry analysis (TGA, Rigaku PTC-10A TG-DTA analyzer).

Electrochemical Measurements.

For electrochemical tests, the working electrodes were comprised of active materials, acetylene black (AB), and polytetrafluoroethylene (PTFE) at the weight ratio of 80 : 10 : 10. The average weight of the electrodes was ~2 mg. In the test cells, lithium metal was used as the counter and reference electrode. The electrolyte was 1 M LiPF₆ dissolved in a 1 : 1 : 1 mixture of ethylene carbonate (EC), ethylene methyl carbonate (EMC) and dimethyl carbonate (DMC). The cells were assembled in a glove box filled with high-purity argon. Discharge/charge tests of

the cells were performed between 0.01-3.0 V (vs. Li/Li⁺) under a LAND-CT2001A instrument at room temperature. CV tests were performed at different scanning rates from 0.1 to 5 mV s⁻¹ between 0.01-3.0 V (vs. Li/Li⁺) after the initial 4 charge/discharge cycles. Electrochemical impedance spectroscopy (EIS) was taken by using an IM6e electrochemical workstation at 25 °C with the frequency range from 10 kHz to 100 mHz and an AC signal of 5 mV in amplitude as the perturbation. The specific capacity was calculated according to the corresponding total weight of active materials in each electrode.

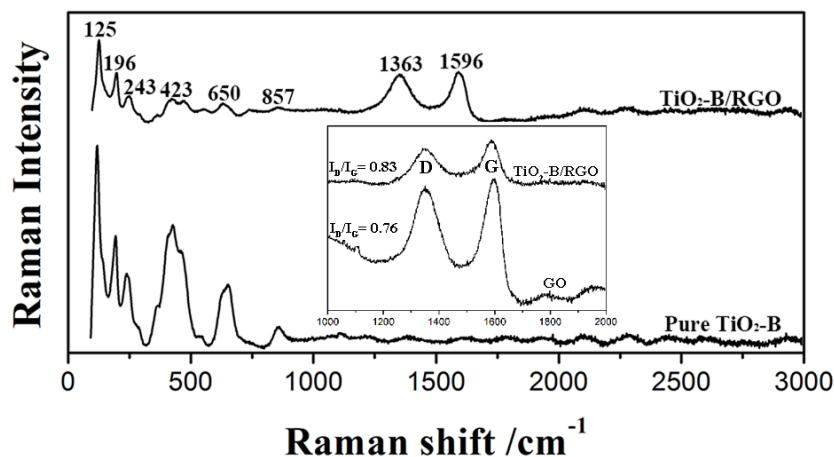


Figure S1. Raman spectra of the as-prepared, GO, TiO₂-B/RGO and pure TiO₂-B.

The Raman spectra were used to characterize the as-prepared GO, pure TiO₂-B and TiO₂-B/RGO composites (Figure S1) for confirming the chemical composition of the samples. The Raman spectrum of GO is characterized by two main features: the G mode arising from the first order scattering of the E_{2g} phonon of sp² C atoms (usually observed at ~1590 cm⁻¹) and the D mode arising from a breathing mode of k-point photons of A_{1g} symmetry (~1358 cm⁻¹).¹ The small value of I_D/I_G ratio (0.76) demonstrates decreased level of disorder which strengthens the electronic conductivity, due to I_D/I_G intensity ratio stands for the disordering degree of GO.² In the case of pure TiO₂-B and TiO₂-B/RGO composites, Raman modes at 125, 196, 243, 423, 650, and 857 cm⁻¹ are characteristic of pure-phase TiO₂-B.³ Compared with the intensity ratio of I_D/I_G of GO (0.76), the intensity ratio of I_D/I_G of the TiO₂-B/RGO composites increases to 0.83, indicating the decrease of the oxygen-functional groups on GO.⁴ In general, the Raman spectra of composites show that RGO and TiO₂-B constitute the composites, which is consistent with the XRD results.

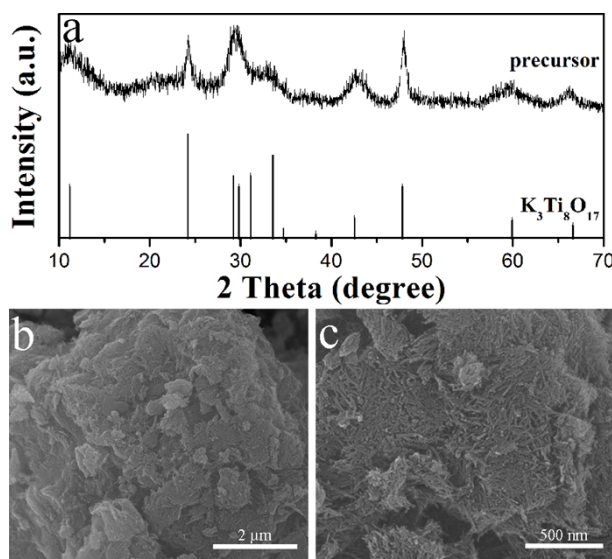


Figure S2. XRD (a) and SEM (b and c) images of the precursor of TiO_2 -B after the first hydrothermal reaction.

The Figure S2a shows the XRD patterns of the precursor of TiO_2 -B after the first hydrothermal reaction, and the peaks of the precursor can be well assigned to the standard card of $\text{K}_3\text{Ti}_8\text{O}_{17}$. The SEM images (Figure S2b and c) show that the precursor is composed of nanorods which have a uniform morphology and small size.

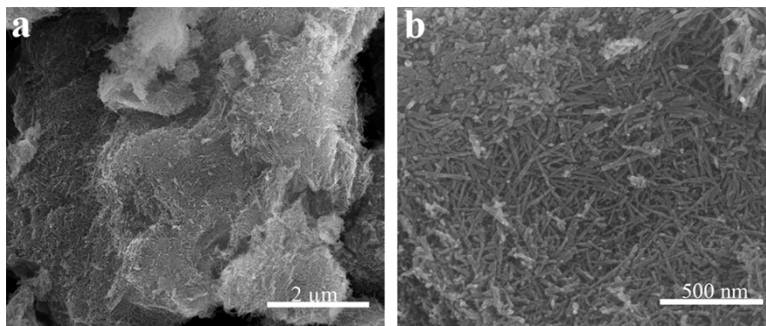


Figure S3. SEM images of pure TiO_2 -B (a and b) and TEM image of as-prepared GO (c and d).

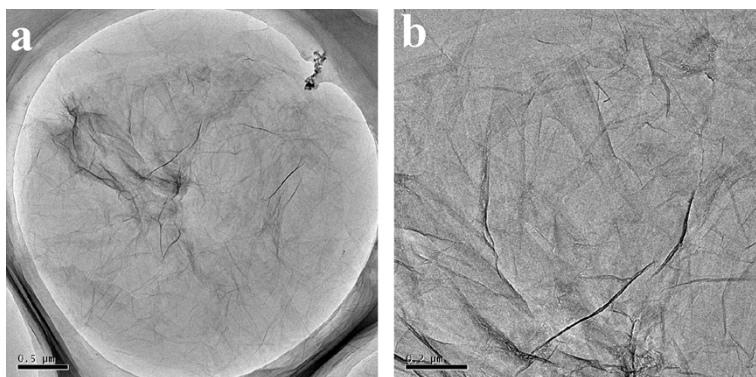


Figure S4. TEM image of as-prepared GO (a and b).

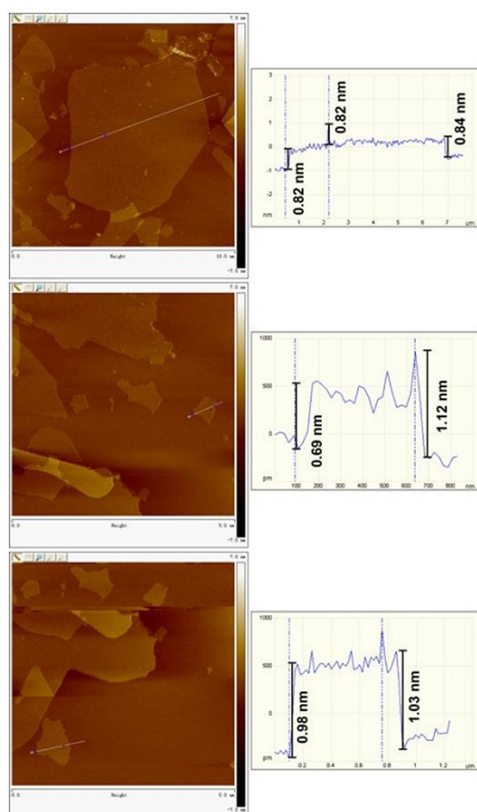


Figure S5. AFM images of GO nanosheets prepared through a modified Hummers' method.

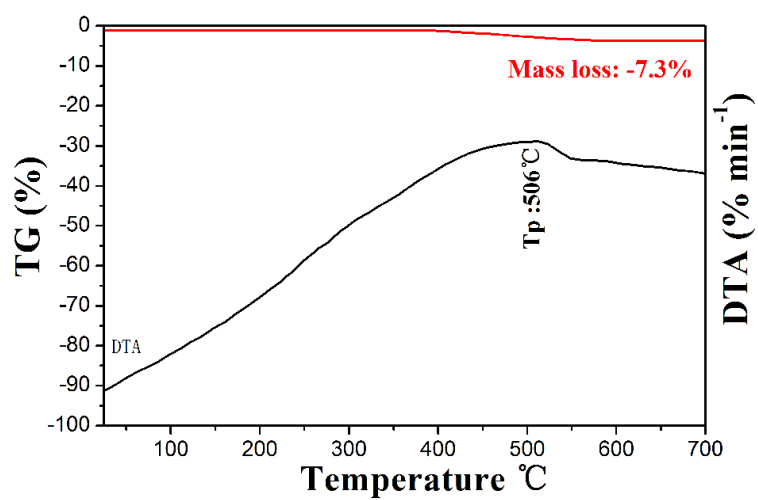


Figure S6. TG-DTA curves of TiO₂-B/RGO nanocomposites in air.

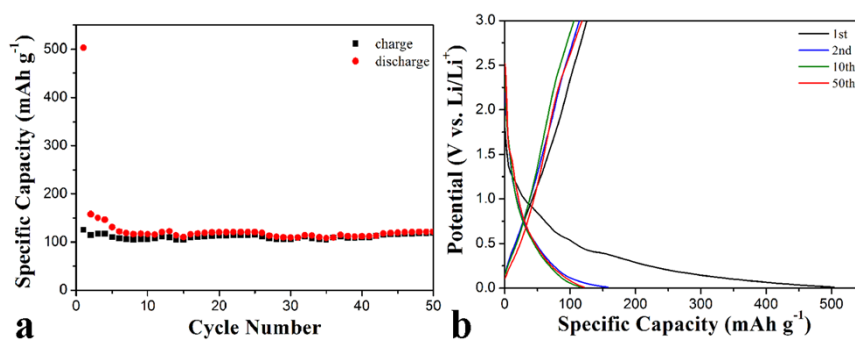


Figure S7. Cyclic performance (a) of pure RGO electrodes at the potential range of 0.001-3.0 V at 1 C (1 C = 335 mA g⁻¹) and discharge/charge profiles (b) of RGO electrodes.

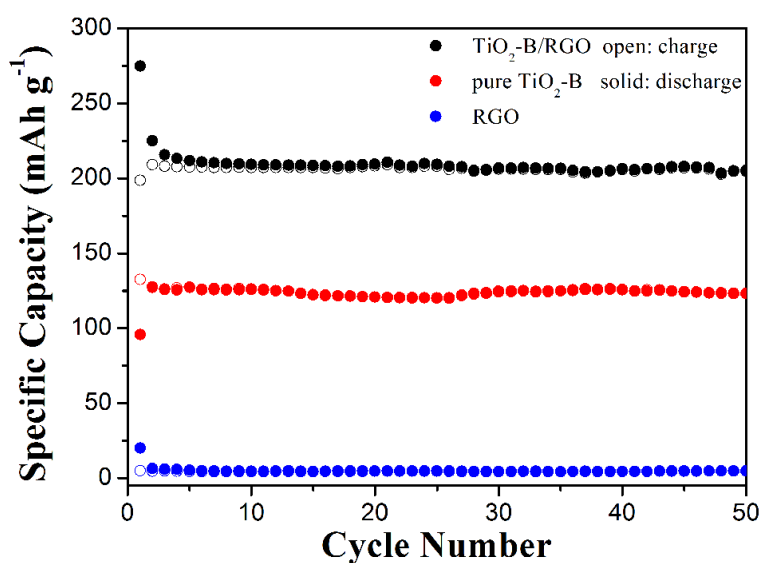


Figure S8. Cyclic performances of TiO₂-B/RGO, pure TiO₂-B and RGO electrodes at the potential range of 1.0-3.0 V at 1C.

The Figure S8 shows that the TiO₂-B/RGO nanocomposites exhibit a higher capacity 205 mAh g⁻¹ at 1 C. Compared with TiO₂-B/RGO nanocomposites, pure TiO₂-B presents a relatively lower higher capacity 122 mAh g⁻¹ at 1 C. RGO electrodes were assembled and tested on the same conditions. When cycled at 1 C, the reversible capacity kept at ~ 5 mAh g⁻¹. Based on its low content (7.3 wt.%) in the composites, the contribution from RGO during 1.0-3.0 V can be neglected, indicating that the synergistic effect of RGO nanosheets and nanostructured TiO₂-B leads to the high reversible capacity of the TiO₂-B/RGO nanocomposites.

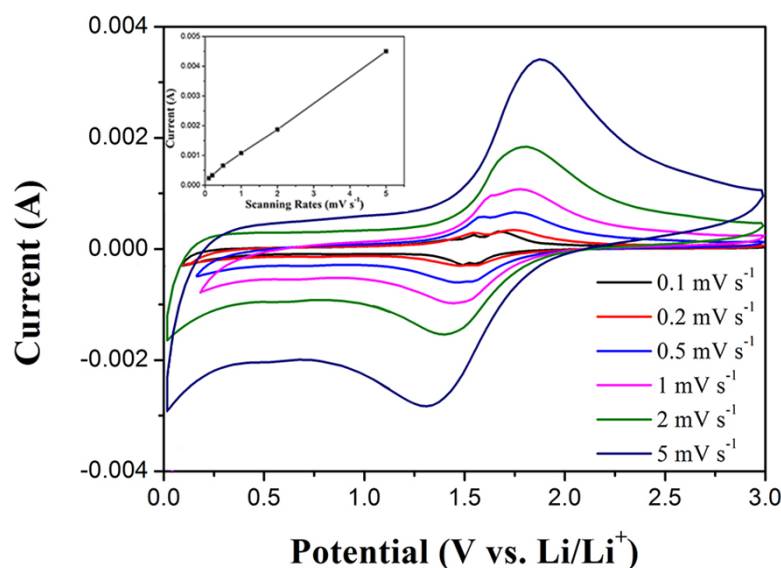


Figure S9. Cyclic voltammograms (CVs) of $\text{TiO}_2\text{-B/RGO}$ composites at different scanning rates after the initial four cycles. Inset: the linear relationship between the peak current densities and scanning rates (in the cathodic process).

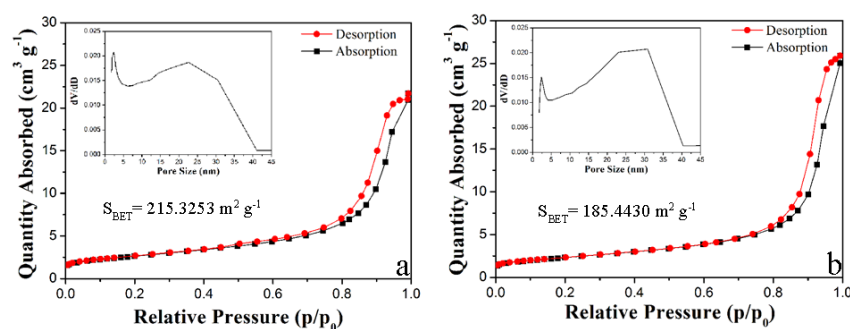


Figure S10. Nitrogen adsorption-desorption isotherms of the $\text{TiO}_2\text{-B/RGO}$ (a) and pure $\text{TiO}_2\text{-B}$ (b) and the pore size distribution (inset).

Notes and references

^aTianjin Key Laboratory of Environmental Remediation and Pollution Control, College of Environmental Science and Engineering, Nankai University, Tianjin 300071, P.R. China.

^bTianjin Key Laboratory of Metal and Molecule Based Material Chemistry, Key Laboratory of Advanced Energy Materials Chemistry (Ministry of Education), Institute of New Energy Material Chemistry, Collaborative Innovation Center of Chemical Science and Engineering (Tianjin), Nankai University, Tianjin 300071, P.R. China.

*Corresponding author. E-mail: liul@nankai.edu.cn; E-mail: zhouzhen@nankai.edu.cn

1. Z. J. Fan, W. Kai, J. Yan, T. Wei, L. J. Zhi, J. Feng, Y. M. Ren, L. P. Song and F. Wei, *ACS Nano*, 2011, **5**, 191-198.
2. H. Huang, J. W. Fang, Y. Xia, X. Y. Tao, Y. P. Gan, J. Du, W. J. Zhu and W. K. Zhang, *J. Mater. Chem. A*, 2013, **1**, 2495-2500.
3. A. G. Dylla, J. A. Lee and K. J. Stevenson, *Langmuir*, 2012, **28**, 2897-2903.
4. J. X. Qiu, P. Zhang, M. Ling, S. Li, P. R. Liu, H. J. Zhao and S. Q. Zhang, *ACS Appl. Mater. Interfaces*, 2012, **4**, 3636-3642.